Synthesis and Characterization of Mixed Ruthenium/Platinum μ_4-Phosphinidene, Phosphorus Monoxide, and Related Clusters

Ludmila Scoles,[†] John H. Yamamoto,[†] Luc Brissieux,[†] Brian T. Sterenberg,[†] Konstantin A. Udachin,[†] and Arthur J. Carty*[,†,‡]

Steacie Institute for Molecular Sciences, National Research Council of Canada, 100 Sussex Drive, Ottawa, Ont., Canada K1A 0R6, and Department of Chemistry, Ottawa-Carleton Chemistry Institute, University of Ottawa, Ottawa, Ontario, Canada K1N 6N5

Received June 18, 2001

The mixed-metal cluster complexes $[Ru_4(CO)_{12}Pt(CO)PPh_3(\mu_4\text{-}PR)]$ [R = N^iPr_2 (**1**), F (**3**)] were formed by capping the Ru_3P face of the nido clusters $[Ru_4(CO)_{13}(\mu_3\text{-}PR)]$ with the labile Pt(0) reagent $[(\eta^2\text{-}C_2H_4)Pt(PPh_3)_2]$. The aminophosphinidene complex **1** undergoes acid hydrolysis to yield the PO complex $[Ru_4(CO)_{12}Pt(CO)PPh_3(\mu_4\text{-}PO)][H_2N^iPr_2]$ (**4**). The fluorophosphinidene cluster **3** reacts with ethanol to form the alkoxyphosphinidene complex $[Ru_4(CO)_{12}Pt(CO)PPh_3(\mu_4\text{-}POEt)]$ (**5**). Comparison of spectroscopic and structural data for clusters **1**, **3**, **4**, and **5** reveals the remarkable effects of the μ_4-phosphinidene and phosphorus monoxide ligands on cluster bonding.

Introduction

Our interest in the synthesis of phosphorus monoxide complexes has been inspired by the fact that free PO has been characterized only spectroscopically in matrices and in molecular beams, but cannot be isolated.[1] Free PO is unstable relative to the higher phosphorus oxides P_4O_6 and P_4O_{10}. Although the chemistry of phosphorus monoxide complexes has grown,[2,3] there is still much to be learned about the coordination properties of PO.

Two synthetic methodologies for the preparation of complexes containing phosphorus monoxide ligands have been described. The first PO complex $[\{\eta^5\text{-}(C_5H^iPr_4)Ni(\mu_3\text{-}PO)\}_2W(CO)_4]$, reported by Scherer et al.,[2] was formed by the direct oxidation of naked phosphide ligands. A similar methodology has been used to prepare several other μ_3-PO clusters and the first η^1-PO complex $[(OP)Mo\{N(R)Ar\}_3]$ [R = $C(CD_3)_2Me$, Ar = 3,5-$C_6H_3Me_2$].[4] This synthetic methodology is limited by the difficulty of accessing the appropriate precursor phosphide complexes.

An alternate and more versatile methodology to access PO clusters was discovered when it was shown that hydrolysis of the aminophosphinidene ligand in $[Ru_4(CO)_{12}(\mu_3\text{-}PN^iPr_2)]$ leads to the anionic PO cluster $[Ru_4(CO)_{12}(\mu_3\text{-}PO)][H_2N^iPr_2]$.[5] We have since extended this strategy, which involves P−N bond cleavage in aminophosphinidene μ_n-PR (R = N^iPr_2, NCy_2) clusters, to the synthesis of a variety of ruthenium and osmium complexes containing μ_3- and μ_4-PO ligands as well as functionalized fluoro-, hydroxy-, and alkoxyphosphinidenes.[6,7]

An attractive approach for the generation of higher nuclearity homonuclear or mixed-metal clusters with phosphinidene or phosphorus monoxide ligands consists of capping the open face of a nido cluster with a metal fragment that contributes the appropriate number of skeletal electrons to convert an $n + 2$ pair nido system to an $n + 1$ skeletal pair closo arrangement. We have previously shown, for example, that treatment of the seven skeletal pair, five vertex nido clusters $[Ru_4(CO)_{13}(\mu_3\text{-}PR)]$ (R = N^iPr_2, NCy_2), which possess an open Ru_3P face, with $Ru(CO)_5$ leads to the closo six vertex molecules $[Ru_5(CO)_{15}(\mu_4\text{-}PR)]$, effectively adding a zero-electron $Ru(CO)_2$ unit to the polyhedron. This cluster was then hydrolyzed to produce the first homonuclear cluster bearing a μ_4-PO ligand.[7a]

We report herein the synthesis and characterization of the first series of mixed-metal (Ru_4Pt) clusters having μ_4-PO, μ_4-PNR_2, μ_4-POR, and μ_4-PF ligands, via the addition of d^{10}-PtL_2 fragments to the Ru_3P face of *nido*-$[Ru_4(CO)_{13}(\mu_3\text{-}PR)]$ (R = N^iPr_2, F), followed by transformations at the phosphinidene ligand.

Experimental Section

Unless specified otherwise, the reactions were carried out under an atmosphere of nitrogen. Hexane, THF, and CH_2Cl_2 were appropriately dried prior to use. The reagents $HBF_4{\cdot}Et_2O$ 54% solution and $[(\eta^2\text{-}C_2H_4)Pt(PPh_3)_2]$ were purchased from Aldrich and used without further purification. The compounds $[Ru_4(CO)_{13}(\mu_3\text{-}PN^iPr_2)]$ and $[Ru_4(CO)_{13}(\mu_3\text{-}PF)]$ were synthesized by known procedures.[5]

[†] National Research Council of Canada.
[‡] University of Ottawa.

(1) (a) Andrews, L.; Withnall, R. *J. Am. Chem. Soc.* **1988**, *110*, 5605. (b) Matthews, H. E.; Feldman, P. A.; Bernath, P. F. *Astrophys. J.* **1987**, *312*, 358.
(2) (a) Scherer, O. J.; Braun, J.; Walther, P.; Heckmann, G.; Wolmershäuser, G.; *Angew. Chem., Int. Ed. Engl.* **1991**, *30*, 852. (b) Scherer, O. J.; Vondung, C.; Wolmershäuser, G. *Angew. Chem., Int. Ed. Engl.* **1997**, *36*, 1303.
(3) (a) Foerstner, J.; Olbrich, F.; Butenschön, H. *Angew. Chem., Int. Ed. Engl.* **1996**, *35*, 1234. (b) Davies, J. E.; Klunduk, M. C.; Mays, M. J.; Raithby, P. R.; Shields, G. P.; Tompkin, P. K.; *J. Chem. Soc., Dalton Trans.* **1997**, 715. (c) Scherer, O. J.; Weigel, S.; Wolmershäuser, G. *Angew. Chem., Int. Ed. Engl.* **1999**, *38*, 3688. (d) Scherer, O. J.; Weigel, S.; Wolmershäuser, G. *Heteroat. Chem.* **1999**, *10*, 622.
(4) Johnson, M. J. A.; Odom, A. L.; Cummins, C. C. *J. Chem. Soc. Chem. Commun.* **1997**, 1523.
(5) (a) Corrigan, J. F.; Doherty, S.; Taylor, N. J.; Carty, A. J. *J. Am. Chem. Soc.* **1994**, *116*, 9799. (b) Wang, W.; Corrigan, J. F.; Doherty, S.; Enright, G. D.; Taylor, N. J.; Carty, A. J. *Organometallics* **1996**, *15*, 2770.
(6) (a) Wang, W.; Carty, A. J. *New J. Chem.* **1997**, *21*, 773. (b) Wang, W.; Enright, G. D.; Carty, A. J. *J. Am. Chem. Soc.* **1997**, *119*, 12370.
(7) (a) Yamamoto, J. H.; Udachin, K. A.; Enright, G. D.; Carty, A. J. *J. Chem. Soc. Chem. Commun.* **1998**, 2259. (b) Yamamoto, J. H.; Scoles, L.; Udachin, K. A.; Enright, G. D.; Carty, A. J. *J. Organomet. Chem.* **2000**, *600*, 84.

10.1021/ic0106423 CCC: $20.00
Published on Web 11/21/2001

TLC separations were performed by using silica gel plates (60 A F_{254}) (Merck, 0.25 mm). Infrared spectra were recorded on a Bio-Rad FTS-40A FTIR spectrometer. The ^{1}H and ^{31}P NMR spectra were obtained on a Bruker DRX-400 spectrometer and the ^{19}F NMR spectra on a Varian Mercury-V • 200 MHz spectrometer. Elemental analyses were performed by Guelph Chemical Laboratories, Guelph, Ontario, Canada.

Reaction of $[Ru_4(CO)_{13}(\mu_3\text{-}PN^iPr_2)]$ with $[(\eta^2\text{-}C_2H_4)Pt(PPh_3)_2]$. $[Ru_4(CO)_{13}(\mu_3\text{-}PN^iPr_2)]$ (73 mg, 0.081 mmol) and $[(\eta^2\text{-}C_2H_4)Pt(PPh_3)_2]$ (68 mg, 0.091 mmol) were dissolved in 10 mL of THF. The resulting red solution was stirred at room temperature for 24 h, at which point the color had changed to red-brown. The solvent was removed in vacuo, and the residue was separated on TLC plates with a mixture of hexane/CH_2Cl_2 (80/20). Three major bands were isolated (orange, brown-green, orange-pink). The bands were determined, in order of elution, to be $[Ru_3(CO)_9Pt(CO)PPh_3(\mu_3\text{-}PN^iPr_2)]$ (**2**) (8 mg, 11%), $[Ru_4(CO)_{12}Pt(CO)PPh_3(\mu_4\text{-}PN^iPr_2)]$ (**1**) (35 mg, 48%), and the known compound $[Ru_3(CO)_{10}(PPh_3)_2]$.[8] All three compounds were crystallized from CH_2Cl_2/hexane at −28 °C over several days.

Data for $[Ru_4(CO)_{12}Pt(CO)PPh_3(\mu_4\text{-}PN^iPr_2)]$ (**1**): IR(CH_2Cl_2), ν(CO): 2075m, 2040vs, 2013s, 1974w cm^{-1}. ^{1}H NMR ($CDCl_3$): δ 7.55−7.4 (m, 15H, C_6H_5), 3.80 (sept, 2H, J_{H-H} = 6.9 Hz, NC*H*(CH_3)$_2$), 1.01(d, 6H, J_{H-H} = 6.9 Hz, NCH(C*H*$_3$)$_2$). ^{31}P{^{1}H} NMR ($CDCl_3$): δ 429.8 (broad, J_{P-Pt} = 968 Hz), 41.36 (d, J_{P-P} = 7 Hz, J_{P-Pt} = 3131 Hz). Anal. Calcd for $Ru_4PtP_2NO_{13}C_{37}H_{29}$: C, 32.75; H, 2.15; N, 1.03. Found: C, 32.20; H, 2.32; N, 1.01.

Data for $[Ru_3(CO)_9Pt(CO)PPh_3(\mu_3\text{-}PN^iPr_2)]$ (**2**): IR, ν(CO) (CH_2Cl_2): 2058w, 2021vs, 1973m, 1932vw cm^{-1}. ^{1}H NMR ($CDCl_3$): δ 7.52−7.38 (m, 15H, C_6H_5), 4.31 (sept, 2H, J_{H-H} = 6.5 Hz, NC*H*(CH_3)$_2$), 1.6 (d, 6H, J_{H-H} = 6.5 Hz, NCH(C*H*$_3$)$_2$). ^{31}P{^{1}H} NMR ($CDCl_3$): δ 459.6 (s), 28.8 (s, J_{P-Pt} = 2726 Hz). Anal. Calcd for $Ru_3PtP_2NO_{10}C_{34}H_{29}$: C, 34.85; H, 2.49; N, 1.2. Found: C, 34.80; H, 2.83; N, 1.17.

Synthesis of $[Ru_4(CO)_{12}Pt(CO)PPh_3(\mu_4\text{-}PF)]$ (3). The cluster $[Ru_4(CO)_{13}(\mu_3\text{-}PF)]$ (60 mg, 0.073 mmol) and $[(\eta^2\text{-}C_2H_4)Pt(PPh_3)_2]$ (120 mg, 0.160 mmol) were dissolved in 10 mL of CH_2Cl_2, resulting in an immediate color change from red to green. The solution was stirred at room temperature for 24 h. The solvent was removed in vacuo and the resulting green solid was separated on TLC plates with the eluting solvent mixture hexane/CH_2Cl_2 (80/20). Three green bands were observed of which only one was successfully characterized. $[Ru_4(CO)_{12}Pt(CO)PPh_3(\mu_4\text{-}PF)]$ (**3**) was isolated by crystallization from CH_2Cl_2/hexane at −28 °C over 3 days. Yield: 20 mg, 33%. IR (CH_2Cl_2), ν(CO): 2086w, 2052vs, 2032vw, 2020m, 1978w cm^{-1}. ^{1}H NMR ($CDCl_3$): δ 7.46−7.54 (m, C_6H_5). ^{31}P{^{1}H} NMR ($CDCl_3$): δ 485.07 (dd, $^2J_{P-P}$ = 11 Hz, $^1J_{P-F}$ = 1095 Hz, $^1J_{P-Pt}$ = 1295 Hz), 32.41 (dd, $^2J_{P-P}$ = 11 Hz, $^3J_{P-F}$ = 20 Hz, $^1J_{P-Pt}$ = 3230 Hz). ^{19}F{^{1}H} NMR ($CDCl_3$, CF_3COOH reference): δ 37.0 (d, $^1J_{F-P}$ = 1095 Hz, $^3J_{P-F}$ = 20 Hz, $^2J_{F-Pt}$ = 26 Hz). Anal. Calcd for $Ru_4PtP_2FO_{13}C_{31}H_{15}$: C, 29.19; H, 1.19. Found: C, 29.21; H, 1.12.

Reaction of $[Ru_4(CO)_{12}Pt(CO)PPh_3(\mu_4\text{-}PN^iPr_2)]$ (1) with HBF_4•H_2O. The cluster $[Ru_4(CO)_{12}Pt(CO)PPh_3(\mu_4\text{-}PN^iPr_2)]$ (**1**, 70 mg. 0.051 mmol) was dissolved in 10 mL of CH_2Cl_2, and an excess of HBF_4•H_2O (0.02 mL of 48% solution) was added. The solution was heated under gentle reflux for 2 days. The solvent was removed in vacuo and the residue was separated on the TLC plates with an 80/20 mixture of hexane and CH_2Cl_2. Two green bands were isolated and were determined to be $[Ru_4(CO)_{12}Pt(CO)PPh_3(\mu_4\text{-}PF)]$ (**3**) (14 mg, 20%) and $[Ru_4(CO)_{12}Pt(CO)PPh_3(\mu_4\text{-}PO)][H_2N^iPr_2]$ (**4**) (12 mg, 17%). Both compounds were crystallized from CH_2Cl_2/hexane at −28 °C. Data for **4**: IR (CH_2Cl_2), ν(CO): 2081w, 2046vs, 2014m, 1972vw cm^{-1}, ν(PO): 1096 cm^{-1}. ^{31}P{^{1}H} NMR ($CDCl_3$): δ 442.4 (d, J_{P-P} = 10 Hz, J_{P-Pt}=1204 Hz), 33.3 (d, J_{P-P} = 10 Hz, J_{P-Pt} = 3177 Hz). FAB-MS (*m*/*z*): 1272 $[M]^+$; 1010 $[M - PPh_3]^+$.

Synthesis of $[Ru_4(CO)_{12}Pt(CO)PPh_3(\mu_4\text{-}POEt)]$ (5). The cluster $[Ru_4(CO)_{12}Pt(CO)PPh_3(\mu_4\text{-}PF)]$ (**3**, 10 mg, 0.0078 mmol) was dissolved in a mixture of CH_2Cl_2 (5 mL) and ethanol (10 mL). The solution was heated under gentle reflux for 2 days. The solvent was removed in vacuo and the solid residue was separated on TLC plates with hexane/CH_2Cl_2 mixture 80/20. One green band was isolated and determined to be $[Ru_4(CO)_{12}Pt(CO)PPh_3(\mu_4\text{-}POEt)]$ (**5**). The product was crystallized from CH_2Cl_2/hexane at −28 °C over 3 days. Yield: 7 mg, 70%. IR (CH_2Cl_2), ν(CO): 2079m, 2045vs, 2013m, 1995sh, 1970vw cm^{-1}. ^{31}P{^{1}H} NMR ($CDCl_3$): δ 460.1 (d, J_{P-P} = 12 Hz, J_{P-Pt} = 1228 Hz), 34.1 (d, J_{P-P} = 12 Hz, J_{P-Pt} = 3159 Hz). ^{1}H NMR ($CDCl_3$): δ 7.6−7.45 (m, 15H), 2.66 (q, 2H, J_{H-H} = 6.8 Hz, C*H*$_2$), 0.57 (t, 3H, J_{H-H} = 6.8 Hz, C*H*$_3$). FAB − MS (*m*/*z*): 1302 $[M]^+$; 1218−1078 $[M - n\text{CO}]^+$ (n = 3−10).

Crystallographic Analysis. Single crystals of compounds **1**−**5** were mounted on a glass fiber with 5-min epoxy. Intensity data were collected on a Siemens SMART CCD diffractometer with the use of graphite-monochromated Mo Kα radiation. Data processing was performed using the SHELXTL package or the NRCVAX package.[9] Neutral atom scattering factors were taken from the standard references.[10] Anomalous dispersions were applied to all non-hydrogen atoms. Lorentz polarization (Lp) and absorption corrections were applied to the data for all the structures. Full matrix least-squares refinements minimized the function $\sum_{hkl} w(|F_o| - |F_c|)^2$, where $w = 1/\sigma(F_o)^2$, $\sigma(F_o) = \sigma(F_o^2)/2F_o$, and $\sigma(F_o^2) = [\sigma(I_{raw})^2 + (0.02I_{net})^2]^{1/2}$/Lp.

All structures were solved by a combination of direct methods and difference Fourier syntheses. All non-hydrogen atoms were refined with anisotropic thermal parameters. Details of data collection, reduction, and results of the analysis are given in Table 1. Compound **1** crystallized in the acentric space group $P2_1$, and the correct enantiomorph was identified via refinement of the absolute structure (Flack) parameter *x*. The parameters in Figure 1 and Table 2 refer to this enantiomorph.

Results and Discussion

Capping Reactions. The 62-electron clusters *nido*-$[Ru_4(CO)_{13}(PR)]$ have been shown to undergo capping reactions with unsaturated organic molecules,[11] main group atoms,[12] and transition metal fragments.[7,13] The core cluster atoms, including the phosphorus atom, form a square-based pyramid with a ruthenium atom at the apex. The open square face thus contains three ruthenium atoms and one phosphorus atom. Reaction of the cluster $[Ru_4(CO)_{13}(PN^iPr_2)]$ with the labile Pt(0) reagent $[(\eta^2\text{-}C_2H_4)Pt(PPh_3)_2]$, which delivers a d^{10}-PtL_2 fragment, results in the capping of this face to form the mixed Pt−Ru cluster $[Ru_4(CO)_{12}Pt(CO)PPh_3(\mu_4\text{-}PN^iPr_2)]$ (**1**). Two other products isolated from the reaction, $[Ru_3(CO)_9Pt(CO)PPh_3(\mu_3\text{-}PN^iPr_2)]$ (**2**) and the $Ru_3(CO)_{12}$ derivative $[Ru_3(CO)_{10}(PPh_3)_2]$, clearly result from cluster degradation (Scheme 1).

An ORTEP diagram of compound **1** is shown in Figure 1. The metal atoms are arranged in a square-based pyramidal geometry with the platinum atom occupying one of the basal sites. The square base is capped with the phosphorus atom of the phosphinidene ligand, resulting in an octahedral arrangement of the six core cluster atoms. The platinum center is bound by one carbonyl and one triphenylphosphine ligand, while each ruthenium center has three terminal carbonyl ligands. The triphenylphosphine ligand on the platinum and the μ_4-PN^iPr_2 ligand lie on the same side of the Ru(1), Ru(2), Ru(3), Pt(1) plane, resulting in an approximately cis arrangement of the two

(8) (a) Chin-Choy, T.; Keder, N. L.; Stucky, G. D.; Ford, P. C. *J. Organomet. Chem.* **1988**, *346*, 225. (b) Bruce, M. I.; Liddell, M. J.; Hughes, C. A.; Patrick, J. M.; Skelton, B. W.; White, A. H. *J. Organomet. Chem.* **1988**, *347*, 181.

(9) Gabe, E. J.; Le Page, Y.; Charland, J. P.; Lee, F. L.; White, P. S. *J. Appl. Crystallogr.* **1989**, *22*, 384.

(10) *International Tables for X-ray Crystallography*; Kynoch: Birmingham, 1975; Vol. IV, pp 99−101.

(11) (a) Corrigan, J. F.; Doherty, S.; Taylor, N. J.; Carty, A. J. *Organometallics* **1992**, *11*, 3160. (b) Corrigan, J. F.; Taylor, N. J.; Carty, A. J. *Chem Commun.* **1991**, 1640.

(12) Van Gastel, F.; Agocs, L.; Cherkas, A. A.; Corrigan, J. F.; Ramachandran, R.; Taylor, N. J.; Carty, A. J. *J. Cluster Sci.* **1991**, *2*, 131.

(13) Blenkiron, P.; Enright, G. D.; Taylor, N. J.; Carty, A. J. Manuscript in preparation.

Table 1. Crystallographic Data for Compounds **1**−**5**

	1	**2**	**3**	**4**	**5**
formula	$Ru_4PtP_2NO_{13}C_{37}H_{29}$	$Ru_3PtP_2NO_{10}C_{34}H_{29}$	$Ru_4PtP_2FO_{13}C_{31}H_{15}$	$Ru_4PtP_2NO_{14}C_{37}H_{31}$	$Ru_4PtP_2O_{14}Cl_{1.4}C_{33.7}H_{21.4}$
formula weight	1356.92	1171.82	1275.74	1374.94	1359.84
crystal system	monoclinic	monoclinic	triclinic	monoclinic	triclinic
lattice parameters					
a (Å)	13.4002(7)	38.717(3)	10.1654(5)	9.8796(6)	13.046(6)
b (Å)	11.4675(6)	10.0918(8)	13.1848(6)	21.0626(12)	13.156(4)
c (Å)	13.7739(8)	20.7789(16)	14.3716(7)	21.3400(12)	13.607(9)
α (deg)	90	90	72.8930(10)	90	83.95(3)
β (deg)	97.01	104.69	88.0520(10)	93.29	86.58(4)
γ (deg)	90	90	85.1390(10)	90	64.96(5)
V (Å^3)	2100.8(2)	7853.5(11)	1834.28(15)	4433.3(4)	2103.9(17)
crystal dimension (mm^{-3})	0.3 × 0.25 × 0.2	0.3 × 0.2 × 0.15	0.3 × 0.25 × 0.15	0.35 × 0.3 × 0.15	0.3 × 0.2 × 0.15
space group	$P2(1)$	$C2/c$	$P\bar{1}$	$P2(1)/n$	$P\bar{1}$
Z	2	8	2	4	2
ρ_{calc} (Mg m^{-3})	2.145	1.982	2.310	2.060	2.147
μ(Mo Kα) (mm^{-1})	4.862	4.818	5.563	4.610	4.942
T (K)	173	173	173	173	173
$2\theta_{max}$ (deg)	57.36	57.38	57.44	57.46	50
reflns measured	19695	45587	21796	52230	14744
unique reflns	10720	10183	9409	11537	7319
observations [$I > 2.5\sigma(I)$]	10720	10183	9409	11537	7319
variables	522	455	469	532	543
goodness of fit	0.802	1.018	0.968	0.937	0.907
residuals: R, R_w	0.0392	0.0337	0.0296	0.0385	0.0538
	0.0542	0.0604	0.0772	0.0654	0.1206
absorption correction	empirical	empirical	empirical	empirical	empirical
largest peak in final difference map (e Å^{-3})	1.281	1.161	1.846	1.081	2.819

phosphorus ligands on the platinum, while the carbonyl is directed away from the phosphinidene. The resulting 74 skeletal electron count is consistent with a seven pair, six-vertex closo octahedral arrangement and an 18-electron platinum center.

The Ru−Ru and Ru−Pt bond lengths fall within the range 2.7627−2.9219 Å. Careful examination of these bond lengths reveals a distortion of the apical Ru(4) atom away from the center of the square toward the Pt−Ru(3) edge. The Ru(4)−Pt [2.7636(7) Å] and Ru(4)−Ru(3) [2.7627(9) Å] are approximately 0.1 Å shorter than the corresponding Ru(4)−Ru(1) [2.9219(8) Å] and Ru(4)−Ru(2) [2.8874(8) Å] distances. The origin of this distortion is unclear. The metal−phosphinidene phosphorus bond lengths also show a distortion. In this case, one distance, P(1)−Ru(3) [2.507(2) Å], is exceptionally long compared to the others [P(1)−Pt = 2.363(2) Å, P(1)−Ru(1) = 2.388(2) Å, P(1)−Ru(2) = 2.381(2) Å].

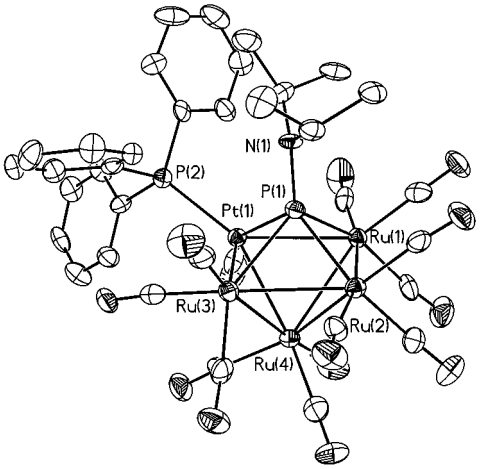

Figure 1. ORTEP diagram of $Ru_4(CO)_{12}Pt(CO)PPh_3(\mu_4\text{-}PN^iPr_2)$ (**1**). Selected bond distances (Å) and angles (deg): Pt(1)−Ru(1) = 2.8929(7), Pt(1)−Ru(3) = 2.8503(7), Pt(1)−Ru(4) = 2.7636(7), Ru(1)−Ru(2) = 2.8160(8), Ru(1)−Ru(4) = 2.9219(8), Ru(2)−Ru(3) = 2.8508(8), Ru(2)−Ru(4) = 2.8874(8), Ru(3)−Ru(4) = 2.7627(9), Pt(1)−P(1) = 2.363(2), Ru(1)−P(1) = 2.388(2), Ru(2)−P(1) = 2.381(2), Ru(3)−P(1) = 2.507(2), Pt(1)−P(2) = 2.349(2), P(1)−N(1) = 1.697(5). P(1)−Pt(1)−P(1) = 148.3(2), P(1)−Pt(1)−C(1) =148.3(2), Ru(1)−Pt(1)−Ru(3) = 91.00(2), Pt(1)−Ru(1)−Ru(2) = 88.10(2), Ru(1)−Ru(2)−Ru(3) = 92.59(2), Ru(2)−Ru(3)−Pt(1) = 88.26(2).

The P(1)−N bond distance in the aminophosphinidene ligand of 1.697(5) Å is comparable to those observed in other μ_4-aminophosphinidene complexes [e.g. 1.681(3) Å in $[Ru_5(CO)_{15}(PNCy_2)]$[7]) and longer than those typically found in μ_3-aminophosphinidene clusters. The Pt−P(2) distance of 2.349(2) Å is a normal Pt−PPh_3 distance.

The ^{31}P NMR spectrum of **1** shows peaks at δ 429.8 and 41.36 for the phosphinidene and phosphine ligands, respectively. The two bond P−P coupling constant is 7 Hz. This small coupling constant reflects the relative cis arrangement of these two ligands on platinum. A ^{195}Pt coupling constant of 3131 Hz is observed in the satellites of the triphenylphosphine resonance, while the ^{195}Pt coupling to the phosphinidene phosphorus atom is much smaller at 968 Hz, reflecting the longer Pt(1)−P(1) bond length [2.363(1) Å vs Pt(1)−P(2) = 2.349(1) Å].

The second mixed-metal product isolated from the reaction is the Ru_3Pt cluster $[Ru_3(CO)_9Pt(CO)PPh_3(\mu_3\text{-}PN^iPr_2)]$ (**2**). An ORTEP diagram of the cluster is shown in Figure 2. The metal atoms form a tetrahedron, and the triangular face of the tetrahedron opposite the platinum atom is capped with the aminophosphinidene ligand, resulting in a trigonal-bipyramidal arrangement of the core cluster atoms, with the ruthenium atoms in the equatorial positions and phosphorus and platinum in the apical positions. Each ruthenium atom is bound by three carbonyls. One carbonyl on each of Ru(1) and Ru(2) forms a semibridging interaction with platinum. On Ru(3), all three carbonyls are terminal. Besides the semibridging carbonyls, the platinum center is also bound by one terminal carbonyl and one triphenylphosphine ligand.

The Ru−Ru distances show a distortion of the Ru_3 triangle, with one long [Ru(1)−Ru(2) = 3.0530(5) Å] and two shorter

Table 2. A Comparison of Spectroscopic and Structural Parameters Involving the Phosphinidene Ligands in $[Ru_4(CO)_{12}Pt(CO)PPh_3(\mu_4\text{-}Pr)]$ [R ≃ N^iPr_2 (**1**), F (**3**), O (**4**), OEt (**5**)]

					d(MM) (Å) [average]		
R	$\delta(^{31}P)\,\mu_4$-PR	$^1J_{Pt-P}$ (Hz)	*d*(Ru−P) (Å)	*d*(Pt−P) (Å)	square	apex	*d*(P1−Ru4) (Å)
N^iPr_2	430	968	2.388(2)	2.363(2)	2.8929(7)	2.7636(7)	3.310
			2.381(2)		2.8503(7)	2.9219(8)	
			2.507(2)		2.8160(8)	2.8874(8)	
					2.8508(8)	2.7627(9)	
					[2.8525]	[2.8339]	
O	442	1204	2.398(1)	2.333(1)	2.8786(5)	2.7550(5)	3.241
			2.349(1)		2.8285(5)	2.8010(6)	
			2.476(1)		2.8651(6)	2.8746(6)	
					2.8263(6)	2.8057(6)	
					[2.8496]	[2.8091]	
OEt	460	1228	2.372(1)	2.299(1)	2.869(1)	2.753(1)	3.051
			2.330(1)		3.000(1)	2.826(1)	
			2.327(1)		2.841(1)	2.896(2)	
					2.872(2)	2.807(1)	
					[2.896]	[2.8205]	
F	485	1295	2.320(1)	2.272(1)	2.9671(4)	2.7574(3)	2.939
			2.302(1)		2.9646(3)	2.8395(5)	
			2.328(1)		2.8633(4)	2.8756(5)	
					2.8898(4)	2.8031(4)	
					[2.9212]	[2.8189]	

Scheme 1

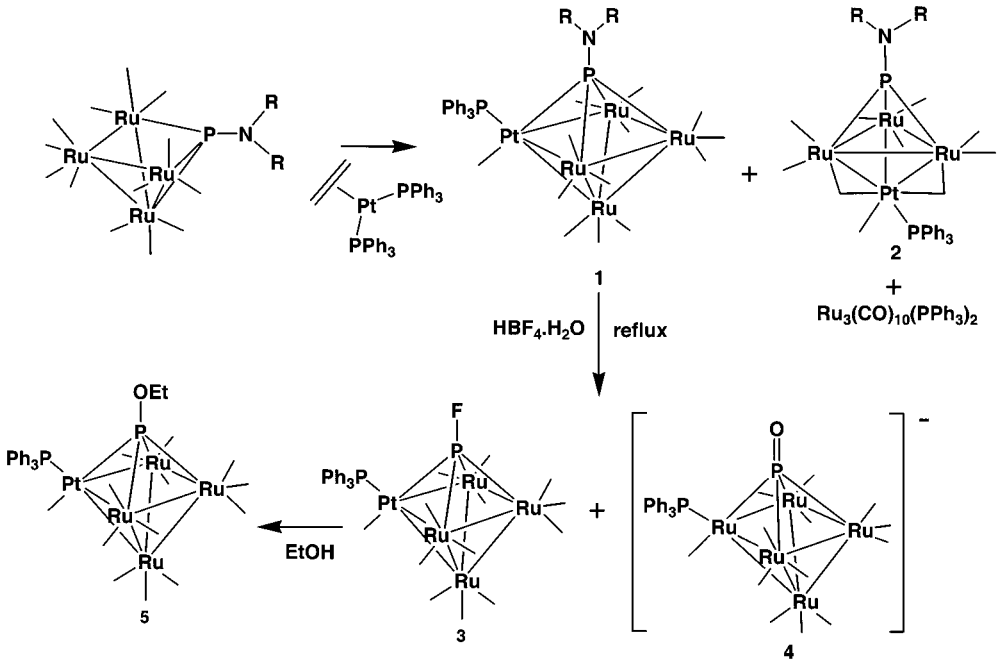

distances [Ru(1)−Ru(3) = 2.8123(5) Å, Ru(2)−Ru(3) = 2.8284(5) Å]. In contrast, the Ru−Pt distances are all very similar, with the unbridged Ru(3)−Pt distance [2.7641(4) Å] being slightly shorter than the carbonyl bridged distances [Ru(2)−Pt = 2.7911(4), Ru(1)−Pt = 2.8064(4) Å]. Ruthenium−phosphorus distances to the phosphinidene ligand are also unsymmetrical, with the longest distance [Ru(3)−P(1) = 2.397-(1) Å] being to the ruthenium atom without semibridging carbonyls. The other distances are approximately equal [Ru-(1)−P(1) = 2.241(1) Å, Ru(2) − P(1) = 2.255(1) Å]. The platinum−carbonyl interactions are clearly semibridging. The Ru−C−O angles [159.8(4)° and 162.4(4)°] are much closer to linearity than the Pt−C−O angles [122.1(4)° and 122.0(4)°] to the same semibridging CO ligands. As well, the Ru−C distances [1.970(5) Å and 1.971(5) Å] are much shorter than the Pt−C distances [2.467(5) Å and 2.531(5) Å]. These parameters confirm that the platinum−semibridging carbonyl interactions are relatively weak and may suggest that the semibridging CO ligands serve to remove electron density from the electron-rich Pt center.

In solution, the infrared spectrum of **2** shows no evidence for bridging carbonyls, with the lowest frequency band occurring at 1932 cm^{-1}. This suggests that the semibridging carbonyls are a solid-state phenomenon or that exchange in solution masks their presence. In the solid state, a weak band is observed at 1733 cm^{-1}. The $^{31}P\{^1H\}$ NMR spectrum of **2** shows peaks at δ 459.6 and 28.8 for the phosphinidene and phosphine ligands, respectively. The chemical shift of the phosphinidene phosphorus nucleus is typical for μ_3-phosphinidenes.[14] There is no P−P coupling and no Pt coupling to the phosphinidene phosphorus

(14) Wang, W.; Corrigan, J. F.; Enright, G. D.; Taylor, N. J.; Carty, A. J. *Organometallics* **1996**, *15*, 2770.

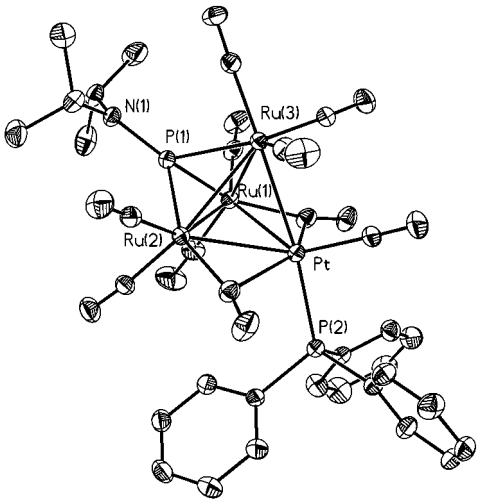

Figure 2. ORTEP diagram of $Ru_3(CO)_9Pt(CO)PPh_3(\mu_3\text{-}PN^iPr_2)$ (**2**). Selected bond distances (Å) and angles (deg): Ru(1)−Ru(2) = 3.0530(5), Ru(1)−Ru(3) = 2.8123(5), Ru(2)−Ru(3) = 2.8284(5), Pt−Ru(1) = 2.8064(4), Pt−Ru(2) = 2.7911(4), Pt−Ru(3) = 2.7641(4), Ru(1)−P(1) = 2.241(1), Ru(2)−P(1) = 2.255(1), Ru(3)−P(1) = 2.397(1), P(1)−N(1) = 1.647(4).

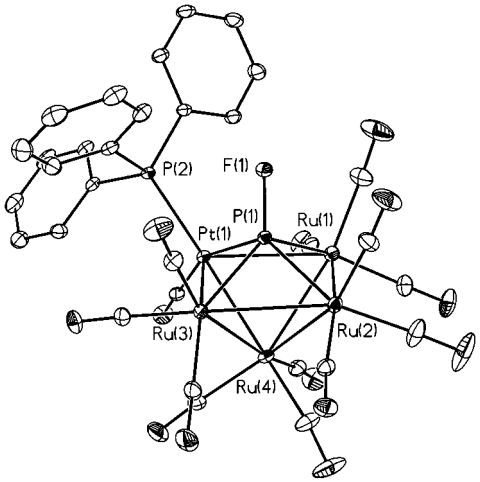

Figure 3. ORTEP diagram of $Ru_4(CO)_{12}Pt(CO)PPh_3(\mu_4\text{-}PF)$ (**3**). Selected bond distances (Å) and angles (deg): Pt(1)−Ru(1) = 2.9671(4), Pt(1)−Ru(3) = 2.9646(3), Pt(1)−Ru(4) = 2.7574(3), Ru(1)−Ru(2) = 2.8633(4), Ru(1)−Ru(4) = 2.8395(5), Ru(2)−Ru(3) = 2.8898(4), Ru(2)−Ru(4) = 2.8756(5), Ru(3)−Ru(4) = 2.8031(4), Pt(1)−P(1) = 2.272(1), Ru(1)−P(1) = 2.320(1), Ru(2)−P(1) = 2.302(1), Ru(3)−P(1) = 2.328(1), Pt(1)−P(2) = 2.3423(9), P(1)−F(1) = 1.610(3). P(1)−Pt(1)−P(1) = 103.58(3), P(1)−Pt(1)−C(1) = 157.5(1), Ru(1)−Pt(1)−Ru(3) = 88.985(9), Pt(1)−Ru(1)−Ru(2) = 89.46(1), Ru(1)−Ru(2)−Ru(3) = 92.53(1), Ru(2)−Ru(3)−Pt(1) = 89.00(1).

atom. The $^{195}Pt-^{31}P$ coupling constant to the phosphine phosphorus atom is 2726 Hz.

The other capping reaction carried out involved the analogous fluorophosphinidene cluster $[Ru_4(CO)_{13}(\mu_4\text{-}PF)]$. Reaction with $[(\eta^2\text{-}C_2H_4)Pt(PPh_3)_2]$ led to the mixed-metal fluorophosphinidene cluster $[Ru_4(CO)_{12}Pt(CO)PPh_3(\mu_4\text{-}PF)]$ (**3**) as the sole isolated product. An ORTEP diagram is shown in Figure 3. Compound **3** is isostructural with compound **1** and shows a similar but smaller distortion of the metal skeleton from the ideal structure. The fluorophosphinidene ligand is almost symmetrically bound, with a slightly shorter distance to Pt [2.272(1) Å] and small variations among P−Ru distances [2.320(1), 2.302(1), 2.328(1) Å]. The P−F distance of 1.610(3) Å is comparable to that seen in other μ_4-fluorophosphinidene clusters recently described [e.g. 1.595(2) Å in $[Ru_5(CO)_{15}(PF)]$[7]].

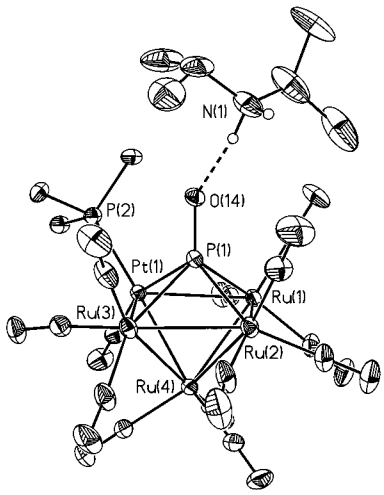

Figure 4. ORTEP diagram of $[Ru_4(CO)_{12}Pt(CO)PPh_3(\mu_4\text{-}PO)][H_2N^i\text{-}Pr_2]$ (**4**), showing the hydrogen-bonding interaction between the anion and cation. Selected bond distances (Å) and angles (deg): Pt(1)−Ru(1) = 2.8786(5), Pt(1)−Ru(3) = 2.8285(5), Pt(1)−Ru(4) = 2.7550(5), Ru(1)−Ru(2) = 2.8651(6), Ru(1)−Ru(4) = 2.8191(6), Ru(2)−Ru(3) = 2.8263(6), Ru(2)−Ru(4) = 2.8746(6), Ru(3)−Ru(4) = 2.8057(6), Pt(1)−P(1) = 2.333(1), Ru(1)−P(1) = 2.398(1), Ru(2)−P(1) = 2.349(1), Ru(3)−P(1) = 2.476(1), Pt(1)−P(2) = 2.344(1), P(1)−O(14) = 1.518(3). P(1)−Pt(1)−P(1) = 100.09(5), P(1)−Pt(1)−C(1) = 160.4(1), Ru(1)−Pt(1)−Ru(3) = 91.57(1), Pt(1)−Ru(1)−Ru(2) = 87.31(1), Ru(1)−Ru(2)−Ru(3) = 91.89(1), Ru(2)−Ru(3)−Pt(1) = 89.04(1).

The ^{31}P resonance of the fluorophosphinidene ligand appears at δ 485 and shows a characteristic $^1J_{P-F}$ of 1094 Hz, as well as platinum satellites ($^1J_{Pt-P}$ = 1295 Hz) and a P−P coupling to the triphenylphosphine phosphorus atom of 11 Hz. The resonance for the triphenylphosphine ligand appears at δ 32.4 with a platinum coupling constant of 3238 Hz, as well as a long-range fluorine coupling of 20 Hz. The fluorine resonance thus appears as a doublet of doublets at δ 37 and also shows a long-range platinum coupling of 26 Hz.

Phosphinidene Ligand Transformations. Having successfully formed mixed platinum−ruthenium amino and fluoro phosphinidene complexes, we were interested in generating the related PO complexes. Unfortunately, the direct route via the capping reaction was not available to us, because the required *nido*- precursor cluster $[Ru_4(CO)_{13}(PO)]^-$ is unstable relative to the *closo*- cluster $[Ru_4(CO)_{12}(PO)]^-$, which is not a good candidate for capping reactions. Instead, we turned to transformation of the phosphinidene ligand. Thus, acid hydrolysis of $[Ru_4(CO)_{12}Pt(CO)PPh_3(\mu_4\text{-}PN^iPr_2)]$ (**1**) with $HBF_4{\cdot}H_2O$ leads to two major products. The first is the fluorophosphinidene complex $[Ru_4(CO)_{12}Pt(CO)PPh_3(\mu_4\text{-}PF)]$ (**3**), described above. The second product is the desired PO complex $[Ru_4(CO)_{12}Pt(CO)PPh_3(\mu_4\text{-}PO)][H_2N^iPr_2]$ (**4**). This reactivity directly parallels that seen in the related Ru_5 system.

An ORTEP diagram of **4** is shown in Figure 4. Compound **4** is isostructural with the aminophosphinidene **1** and the fluorophosphinidene **3** and contains an octahedral arrangement of the core cluster atoms, with the μ_4-phosphorus monoxide ligand capping an Ru_3Pt square. Thus **4** is the first mixed-metal cluster with a μ_4-PO ligand. Like the fluorophosphinidene cluster **3**, distortion from the ideal geometry is much less pronounced than in the aminophosphinidene complex.

Examination of packing diagrams clearly shows the presence of hydrogen bonding between the diisopropylammonium counterion and the oxygen atom of the phosphorus monoxide ligand, with an O···H contact of 1.814 Å. Such hydrogen bonding to ammonium counterions has been observed in other PO com-

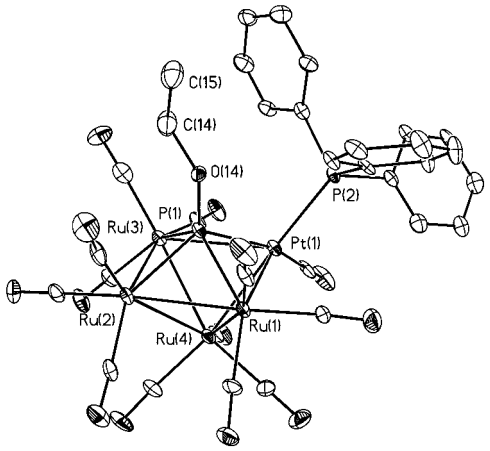

Figure 5. ORTEP diagram of $Ru_4(CO)_{12}Pt(CO)PPh_3(\mu_4\text{-POEt})$ (**5**). Selected bond distances (Å) and angles (deg): Pt(1)−Ru(1) = 2.869(1), Pt(1)−Ru(3) = 3.000(1), Pt(1)−Ru(4) = 2.753(1), Ru(1)−Ru(2) = 2.841(1), Ru(1)−Ru(4) = 2.826(1), Ru(2)−Ru(3) = 2.872(2), Ru(2)−Ru(4) = 2.896(2), Ru(3)−Ru(4) = 2.807(1), Pt(1)−P(1) = 2.299(1), Ru(1)−P(1) = 2.372(1), Ru(2)−P(1) = 2.330(1), Ru(3)−P(1) = 2.327(1), Pt(1)−P(2) = 2.337(1), P(1)−O(14) = 1.587(1). P(1)−Pt(1)−P(1) = 103.42(3), P(1)−Pt(1)−C(1) = 155.49(5), Ru(1)−Pt(1)−Ru(3) = 99.97(5), Pt(1)−Ru(1)−Ru(2) = 91.03(5), Ru(1)−Ru(2)−Ru(3) = 92.13(5), Ru(2)−Ru(3)−Pt(1) = 87.83(5).

plexes formed using this methodology. The PO bond distance of 1.518(3) Å compares well with the PO bond distance of 1.516(4) Å in $[Ru_5(CO)_{15}(PO)][H_2NCy_2]$, which also shows substantial hydrogen bonding between the PO oxygen atom and the ammonium counterion.[7] The PO stretching frequency is observed at 1095 cm^{-1}, compared with 1063 cm^{-1} in $[Ru_5(CO)_{15}(PO)][H_2N^iPr_2]$.

The reactivity of the fluorophosphinidene complex $[Ru_4(CO)_{12}Pt(CO)PPh_3(\mu_4\text{-PF})]$ (**3**) has been demonstrated by reaction with ethanol, which results in displacement of fluoride by the ethoxy group, forming the ethoxyphosphinidene complex $[Ru_4(CO)_{12}Pt(CO)PPh_3(\mu_4\text{-POEt})]$ (**5**). An ORTEP diagram of **5** is shown in Figure 5. The cluster is isostructural with the other Ru_4Pt clusters. Of note is the longer P−O distance of 1.587(1) Å, which is at the lower end of the range of values found in trialkyphosphites [e.g. P−O = 1.595(19) Å in $(MeO)_3P$ complexes[15]] but somewhat shorter than values in $[Ru_4(CO)_{13}(\mu_3\text{-POMe})]$ [1.613(3) Å][7b] and $[Ru_5(CO)_{15}(\mu_4\text{-POMe})]$ [1.609(2) Å].[6a] A comparison with the P−O distance in $[Ru_4(CO)_{12}Pt(CO)PPh_3(\mu_4\text{-PO})][H_2N^iPr_2]$ (**4**) of 1.518(3) Å clearly shows the higher multiple character of the P−O bond in the phosphorus monoxide cluster.

The ^{31}P resonance of the ethoxyphosphinidene ligand appears at δ 460 with a 1228 Hz coupling to ^{195}Pt and a phosphorus−phosphorus coupling constant of 12 Hz. The triphenylphosphine resonance appears at δ 34.1.

Some remarkable correlations of ^{31}P chemical shifts, $^{31}P-^{195}Pt$ coupling constants, and M−P and M−M bond lengths have been observed in this series of clusters. For example, a comparison of the chemical shifts of all of the related phosphinidene clusters reveals a clear trend. As the electronegativity of the group on phosphorus increases, the phosphorus chemical shift moves further downfield (see Table 2). This trend is the same as that observed in the $Ru_5(CO)_{15}PR$ and $Ru_4(CO)_{13}PR$ series of clusters[6a,7b] and reflects a decrease in shielding at phosphorus as electronegativity increases. A parallel trend is observed in the phosphinidene phosphorus−platinum coupling constants, which increase as the electronegativity of the phosphorus substituent increases. The platinum−phosphorus bond distances show the opposite but consistent effect, decreasing as the electronegativity of the substituent increases, as do the platinum−ruthenium distances. Examination of the metal−metal bond distances reveals another significant change. While the distances to the apical Ru atom do not vary significantly as the phosphinidene ligand is changed, the bonds within the Pt−Ru(1)−Ru(2)−Ru(3) square become significantly longer as the electronegativity of the substituent increases. Combined with the shortening of the metal−phosphorus bonds, the net effect is a compression along the *z*-axis and expansion along the *x*- and *y*-axes as the electronegativity increases. That is, the phosphinidene phosphorus atom moves closer to the apical ruthenium atom (see P1−Ru4 distances in Table 2).

It is thus apparent that an increase in the electronegativity of the substituent on phosphorus results in an increase in the strength of the bonds between the metals and the phosphorus atom of the phosphinidene ligand. The increased electronegativity of the substituents on phosphorus results in a contraction of the phosphorus valence orbitals, including the 3d orbitals,[16] thus enhancing metal−phosphorus $d\pi-d\pi$ overlap.[17] An increased transfer of electron density to phosphorus results in a weakening of the metal−metal bonds in the Ru_3Pt square. The lack of change in bonding to the apical ruthenium atom [Ru(4) in the figures] suggests that there is little competition for electron density between the phosphinidene and the apical metal−metal bonds. In fact, the compression along the *z*-axis in the cluster may indicate an enhancement of through-the-cluster ruthenium−phosphorus bonding, similar to that calculated theoretically in bis(phosphinidene) clusters such as $Fe_4(CO)_{12}(\mu_4\text{-PR})_2$.[17a]

Conclusions

A combination of capping reactions and phosphinidene ligand transformations has been used to synthesize a series of mixed-metal substituted phosphinidene clusters and the first mixed-metal cluster containing quadruply bridging phosphorus monoxide. The octahedral, 74 skeletal electron clusters contain μ_4-substituted phosphinidene ligands, and comparison of the structural and spectroscopic properties of the ligands clearly demonstrates the influence of the phosphinidene substituent on metal−phosphorus and metal−metal bonding as well as on ^{31}P chemical shifts and $^{31}P-^{195}Pt$ coupling constants.

Acknowledgment. This work was supported by funding from the National Research Council of Canada and the Natural Sciences and Engineering Research Council of Canada (to A.J.C.).

Supporting Information Available: Full details of the crystal structure analyses for compounds **1**−**5**, including tables of bond distances and angles, atomic coordinates, and anisotropic thermal parameters. This material is available free of charge via the Internet at http://pubs.acs.org.

IC0106423

(15) Orpen, A. G.; Brammer, L.; Allen, F. H.; Kennard, O.; Watson, D. G.; Taylor, R. *J. Chem. Soc., Dalton Trans.* **1989**, S1.

(16) Albright, T. A.; Burdett, J. K.; Whangbo, M.-H. *Orbital Interaction in Chemistry*; John Wiley & Sons: New York, 1985.

(17) For detailed descriptions of the bonding in phosphinidene and phosphorus monoxide clusters, see: (a) Halet, J.-F.; Hoffmann, R.; Saillard, J.-Y. *Inorg. Chem.* **1985**, *24*, 1695. (b) Kahlal, S.; Udachin, K. A.; Scoles, L.; Carty, A. J.; Saillard, J.-Y. *Organometallics* **2000**, *19*, 2251. (c) Bérces, A.; Koentjoro, O.; Sterenberg, B. T.; Yamamoto, J. H.; Tse, J.; Carty, A. J. *Organometallics* **2000**, *19*, 4336.